



# The Two-Component Signal Transduction System VxrAB Positively Regulates *Vibrio cholerae* Biofilm Formation

Jennifer K. Teschler, Andrew T. Cheng, Fitnat H. Yildiz

Department of Microbiology and Environmental Toxicology, University of California, Santa Cruz, Santa Cruz, California, USA

**ABSTRACT** Two-component signal transduction systems (TCSs), typically composed of a sensor histidine kinase (HK) and a response regulator (RR), are the primary mechanism by which pathogenic bacteria sense and respond to extracellular signals. The pathogenic bacterium *Vibrio cholerae* is no exception and harbors 52 RR genes. Using in-frame deletion mutants of each RR gene, we performed a systematic analysis of their role in *V. cholerae* biofilm formation. We determined that 7 RRs impacted the expression of an essential biofilm gene and found that the recently characterized RR, VxrB, regulates the expression of key structural and regulatory biofilm genes in *V. cholerae*. *vxB* is part of a 5-gene operon, which contains the cognate HK *vxA* and three genes of unknown function. Strains carrying  $\Delta vxA$  and  $\Delta vxB$  mutations are deficient in biofilm formation, while the  $\Delta vxC$  mutation enhances biofilm formation. The overexpression of VxrB led to a decrease in motility. We also observed a small but reproducible effect of the absence of VxrB on the levels of cyclic di-GMP (c-di-GMP). Our work reveals a new function for the Vxr TCS as a regulator of biofilm formation and suggests that this regulation may act through key biofilm regulators and the modulation of cellular c-di-GMP levels.

**IMPORTANCE** Biofilms play an important role in the *Vibrio cholerae* life cycle, providing protection from environmental stresses and contributing to the transmission of *V. cholerae* to the human host. *V. cholerae* can utilize two-component systems (TCS), composed of a histidine kinase (HK) and a response regulator (RR), to regulate biofilm formation in response to external cues. We performed a systematic analysis of *V. cholerae* RRs and identified a new regulator of biofilm formation, VxrB. We demonstrated that the VxrAB TCS is essential for robust biofilm formation and that this system may regulate biofilm formation via its regulation of key biofilm regulators and cyclic di-GMP levels. This research furthers our understanding of the role that TCSs play in the regulation of *V. cholerae* biofilm formation.

**KEYWORDS** *Vibrio cholerae*, VxrAB, biofilms, c-di-GMP, motility

*Vibrio cholerae* is the causative agent of the gastrointestinal disease cholera, responsible for approximately 3 to 5 million cases of severe diarrhea and 120,000 deaths annually (1, 2). A resident of aquatic reservoirs, *V. cholerae* can be found as free-swimming planktonic cells or in matrix-protected cellular aggregates, known as biofilms (2–4). Evidence suggests that biofilms form during the aquatic and intestinal phases of the *V. cholerae* life cycle and play an important role in environmental survival, as well as in the intestinal and transmission stages of infection (5–9). *V. cholerae* biofilm formation requires the production and secretion of an extracellular matrix composed of matrix proteins, nucleic acids, and *Vibrio* polysaccharide (VPS), a glycoconjugate that is essential for the formation of three-dimensional biofilm structures (10–16). A complex regulatory network governs this process, tightly controlling *V. cholerae* biofilm produc-

Received 2 March 2017 Accepted 5 June 2017

Accepted manuscript posted online 12 June 2017

**Citation** Teschler JK, Cheng AT, Yildiz FH. 2017. The two-component signal transduction system VxrAB positively regulates *Vibrio cholerae* biofilm formation. *J Bacteriol* 199:e00139-17. <https://doi.org/10.1128/JB.00139-17>.

**Editor** Igor B. Zhulin, University of Tennessee at Knoxville

**Copyright** © 2017 American Society for Microbiology. All Rights Reserved.

Address correspondence to Fitnat H. Yildiz, [fyildiz@ucsc.edu](mailto:fyildiz@ucsc.edu).

J.K.T. and A.T.C. contributed equally to this article.

tion. While important biofilm regulators and their genetic interactions have been examined, relatively little is known about how environmental signals are integrated into the biofilm regulatory network (8, 17–19).

Like most pathogenic bacteria, *V. cholerae* utilizes two-component signal transduction systems (TCSs) as a means for sensing and responding to different environment stimuli, such as nutrient availability, pH, oxygen, osmolarity, quorum sensing signals, and numerous host factors (19–23). The genome of *V. cholerae* is predicted to encode 43 histidine kinases (HKs) and 49 response regulators (RRs), according to the reference genome of O1 EL Tor strain N16961 ([http://www.ncbi.nlm.nih.gov/Complete\\_Genomes/RRcensus.html](http://www.ncbi.nlm.nih.gov/Complete_Genomes/RRcensus.html) and <http://www.p2cs.org>). An additional 3 RR (VpsT, VpsR, and VC0396) were identified based on an analysis of the genome for REC domains; thus, it is predicted that the *V. cholerae* O1 EL Tor N16961 genome encodes 53 putative RRs. Only 9 RRs have been previously shown to impact biofilm formation. VpsR, VpsT, and LuxO are activators of biofilm formation, while PhoB, VarA, VieA, and CarR are repressors of biofilm formation (22, 24–31). VC1348 and VCA0210 are RRs that contain HD-GYP domains with predicted cyclic di-GMP (c-di-GMP) phosphodiesterase activity. Overexpression of these RRs led to a significant decrease in biofilm formation (32). To date, there is no systematic analysis reporting on the contribution of each TCS to biofilm formation in *Vibrio cholerae*.

Here, we report our results for the analysis of *vpsL* expression, as a representative biofilm gene, in strains with in-frame deletions of each RR. We found that VxrB, an RR that we recently characterized for its roles in intestinal colonization and in regulation of the type 6 secretion system (T6SS) (33), was also a positive regulator of biofilm formation.

## RESULTS

**The VxrB RR is a newly identified positive regulator of *vps* expression in *V. cholerae*.** To assess the role of *V. cholerae* TCSs in biofilm formation, we utilized an in-frame deletion mutant library of 41 response regulators (RR). In this study, the 11 RRs that were predicted to be involved in chemotaxis (CheY, CheV, and CheB proteins) and VC2368 (which we were unable to generate an in-frame deletion for) were not included (34, 35). VPS is required for biofilm formation, and *vps* transcription is a useful readout of potential biofilm forming capacity. Therefore, we analyzed the expression of *vpsL*, the first gene in the *vps*-II cluster, which, along with the *vps*-I cluster genes, encodes components that are required for VPS production and biofilm formation. We used a transcriptional fusion of the regulatory region of *vpsL* and the luciferase transcriptional reporter *luxCADBE* ( $P_{vpsL}$ -*lux*). Our results revealed 7 RR-null mutants with significant changes in *vpsL* expression compared with that in the wild type (Fig. 1). Consistent with previous studies, we observed a 122-fold decrease in *vpsL* expression in the  $\Delta vpsR$  (VC0665) strain, an 81-fold decrease in *vpsL* expression in the  $\Delta luxO$  (VC1021) strain, an 11-fold decrease in *vpsL* expression in the  $\Delta vpsT$  (VCA0952) strain, and a 4-fold increase in *vpsL* expression in the  $\Delta carR$  (VC1320) strain (24, 27, 28). A 3-fold increase in *vpsL* expression was observed in the  $\Delta ntrC$  (VC2749) strain, indicating that this RR may be a repressor of biofilm formation. Additionally, we observed a 47-fold decrease in *vpsL* expression in a  $\Delta varA$  (VC1213) mutant. Furthermore, we found that the  $\Delta vxrB$  (VCA0566) strain had an 11-fold decrease in *vpsL* expression, indicating that this RR may be a positive regulator of biofilm formation (Fig. 1). Since VxrB was not previously reported to be a regulator of biofilm, we focused this work on characterizing how this TCS influences biofilm formation.

We recently determined that VxrB, along with its cognate sensor histidine kinase (HK), VxrA, regulates the type VI secretion system (T6SS) and virulence (33). Another recent study additionally showed that the VxrAB TCS plays a role in cell wall homeostasis in response to antibiotic treatment (in that study, the authors renamed VxrAB as WigKR) (36). However, this is the first report of its role in the regulation of biofilm-gene expression. To further characterize the role of the VxrAB TCS in *vpsL* regulation, we analyzed *vpsL* expression in the  $\Delta vxrA$  strain. We observed that, similar to that with

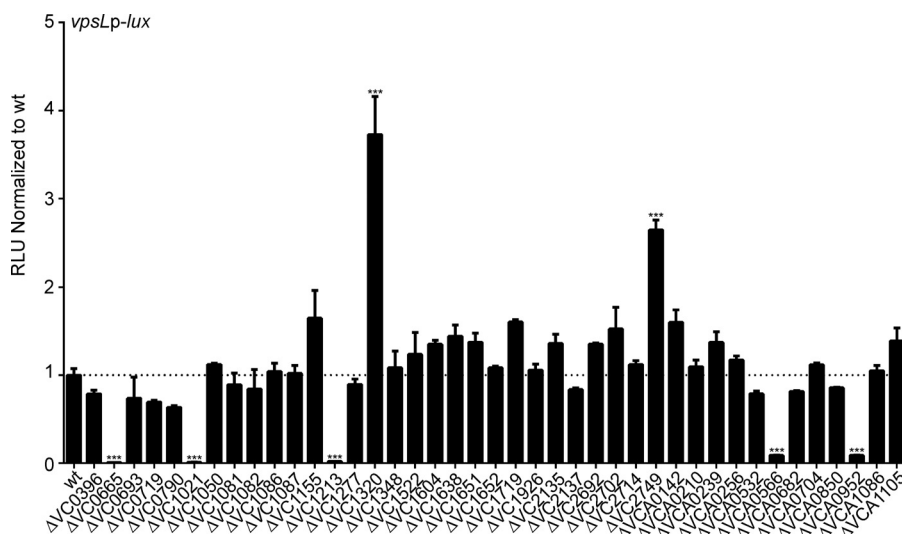


**FIG 1** Analysis of biofilm gene expression in the wild type and in response regulator (RR) deletion mutants. A transcriptional reporter harboring the regulatory region of *vpsL* upstream of a promoterless *lux* reporter ( $P_{vpsL}$ -*lux*) was used to analyze the expression of biofilm genes in 41  $\Delta$ RR mutants, including  $\Delta$ VCA0396 (*gstR*),  $\Delta$ VCA0665 (*vpsR*),  $\Delta$ VCA0693,  $\Delta$ VCA0719 (*phoB*),  $\Delta$ VCA0790,  $\Delta$ VCA1021 (*luxO*),  $\Delta$ VCA1050,  $\Delta$ VCA1081,  $\Delta$ VCA1082,  $\Delta$ VCA1086,  $\Delta$ VCA1087,  $\Delta$ VCA1155,  $\Delta$ VCA1213 (*varA*),  $\Delta$ VCA1277,  $\Delta$ VCA1320 (*carR*),  $\Delta$ VCA1348,  $\Delta$ VCA1522,  $\Delta$ VCA1604,  $\Delta$ VCA1638,  $\Delta$ VCA1651 (*vieB*),  $\Delta$ VCA1652 (*vieA*),  $\Delta$ VCA1719 (*torR*),  $\Delta$ VCA1926 (*dctD1*),  $\Delta$ VCA2135 (*ftrC*),  $\Delta$ VCA2137 (*ftrA*),  $\Delta$ VCA2692 (*cpxR*),  $\Delta$ VCA2702 (*cbrR*),  $\Delta$ VCA2714 (*ompR*),  $\Delta$ VCA2749 (*ntnC*),  $\Delta$ VCA0142 (*dctD2*),  $\Delta$ VCA0210,  $\Delta$ VCA0239,  $\Delta$ VCA0256,  $\Delta$ VCA0532,  $\Delta$ VCA0566 (*vxB*),  $\Delta$ VCA0682 (*uhpA*),  $\Delta$ VCA0704 (*pgtA*),  $\Delta$ VCA0850,  $\Delta$ VCA0952 (*vpsT*),  $\Delta$ VCA1086, and  $\Delta$ VCA1105 strains (names included in parentheses where relevant). Cultures of the wild type and  $\Delta$ RR mutants were grown to exponential phase ( $OD_{600}$  of  $\sim 0.3$ ) and luminescence was measured. The graph represents the averages and standard deviations of relative light units (RLU) obtained from at least three technical replicates from two biological replicates, normalized to wild-type levels. RLU are reported in luminescence counts  $\cdot$  min $^{-1}$   $\cdot$  ml $^{-1}$   $\cdot$   $OD_{600}^{-1}$ . These values were then normalized to the wild-type RLU, and data are shown as fold changes above or below a wild-type value of 1. Data were analyzed using a one-way analysis of variance (ANOVA) and Bonferroni's multiple-comparison test. \*\*\*,  $P < 0.001$ .

$\Delta$ *vxB* deletion, a  $\Delta$ *vxB* mutant downregulates expression of *vpsL* by 3-fold. A  $\Delta$ *vxB* strain harboring *vxB* under the control of its own promoter ( $P_{vxB}$ ) in the Tn7 site was complemented for *vpsL* expression (Fig. 2A). These results demonstrate that the VxrAB TCS positively regulates *vpsL* gene expression.

**VxrB acts upstream of the major biofilm regulators, VpsR and VpsT.** The two major positive regulators of *vps* genes are VpsR and VpsT. To determine if VxrB affects the regulators of *vps* gene expression, we measured the expression of each regulator in the  $\Delta$ *vxB* strain using the transcriptional fusions  $P_{vpsR}$ -*lux* and  $P_{vpsT}$ -*lux*. Expression of *vpsL*, *vpsR*, and *vpsT* was decreased by 4-fold, 2.5-fold, and 3-fold, respectively, in the  $\Delta$ *vxB* strain compared with that in the wild type, suggesting that VxrB could regulate *vpsL* expression by activating the expression of *vpsR* and *vpsT* (Fig. 2B). A  $\Delta$ *vxB* strain harboring *vxB* under the control of its own promoter ( $P_{vxB}$ ) in the Tn7 site was complemented for *vpsR* and *vpsT* expression (Fig. 2B).

We performed an epistasis analysis with *vpsR*, *vpsT* and *vxB*. Our results revealed that the deletion of *vxB* in the  $\Delta$ *vpsR* or  $\Delta$ *vpsT* strain had no significant effect on *vpsL* expression compared with that in the single mutants ( $\Delta$ *vpsR* and  $\Delta$ *vpsT* strains) (Fig. 3A). These data suggest that VpsR and VpsT function downstream of VxrB for *vpsL* expression. Given that VpsR is at the bottom of the *vps* regulatory cascade, we reasoned that VxrB-dependent regulation of *vpsL* might ultimately be due to increased expression of *vpsR*. To test this, we expressed *vpsR* (inserted in the Tn7 site) from an isopropyl- $\beta$ -D-1-thiogalactopyranoside (IPTG) inducible promoter and analyzed *vpsL* expression in wild-type (WT),  $\Delta$ *vxB*, and  $\Delta$ *vxB* strains. We observed that *vpsL* expression was increased by 11-fold when *vpsR* was overexpressed in the wild type. The overexpression of *vpsR* in the  $\Delta$ *vxB* or  $\Delta$ *vxB* strain also resulted in increased *vpsL* expression, although

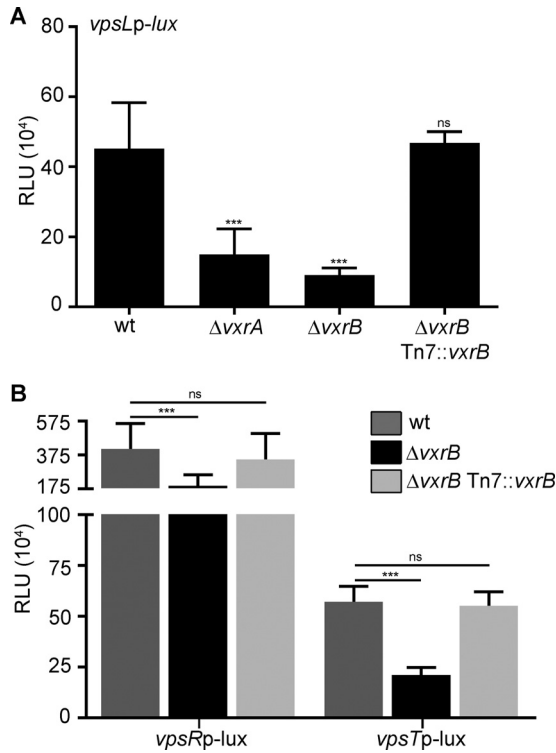


**FIG 2** Analysis of biofilm gene expression in the wild type and in  $\Delta vxrA$  and  $\Delta vxrB$  mutants. (A) Cultures of wild-type,  $\Delta vxrA$ ,  $\Delta vxrB$ , and  $\Delta vxrB$  Tn7:: $vxrB$  strains containing  $P_{vpsL}$ - $lux$  were grown to exponential phase ( $OD_{600}$  of  $\sim 0.3$ ) and luminescence was measured. The graph represents the averages and standard deviations of RLU obtained from three technical replicates from three biological replicates. RLU are reported in luminescence counts  $\cdot$  min<sup>-1</sup>  $\cdot$  ml<sup>-1</sup>  $\cdot$  OD<sub>600</sub><sup>-1</sup>. Data were analyzed using a one-way analysis of variance (ANOVA) and Bonferroni's multiple-comparison test. \*\*\*,  $P < 0.001$ ; ns, not significant. (B) Cultures of wild-type and  $\Delta vxrB$  strains containing  $P_{vpsR}$ - $lux$  or  $P_{vpsT}$ - $lux$  were grown to exponential phase ( $OD_{600}$  of  $\sim 0.3$ ) and luminescence was measured. The graph represents the averages and standard deviations of RLU obtained from three technical replicates from three biological replicates. RLU are reported in luminescence counts  $\cdot$  min<sup>-1</sup>  $\cdot$  ml<sup>-1</sup>  $\cdot$  OD<sub>600</sub><sup>-1</sup>. Data were analyzed using two-tailed Student's  $t$  tests. \*\*\*,  $P < 0.0001$ .

$\sim 5$ -fold less than in the wild type. Taken together, these results suggest that VxrB can regulate  $vpsL$  expression independently of VpsR.

**Members of the  $vxr$  operon affect  $vps$  expression and biofilm formation.** The VxrAB TCS is encoded as part of a 5-gene operon, composed of the HK  $vxrA$ , the RR  $vxrB$ , and three genes of unknown function,  $vxrC$ ,  $vxrD$ , and  $vxrE$  (Fig. 4A). We previously demonstrated that the  $vxrABCDE$  genes are cotranscribed (33). To characterize the role of  $vxr$  genes in biofilm formation, we analyzed  $vpsL$  expression normalized to total protein in mutants lacking  $vxr$  operon genes (Fig. 4B). For this study, we analyzed  $P_{vpsL}$ - $lux$  in biofilm-grown cells. As demonstrated above, the  $\Delta vxrA$  and  $\Delta vxrB$  strains both had decreased  $vpsL$  expression compared with that in the wild type. The  $\Delta vxrC$  mutant showed a 1.5-fold increase in  $vpsL$  expression compared with the wild type, while the  $\Delta vxrD$  and  $\Delta vxrE$  strains showed a 3-fold and 4-fold decrease in  $vpsL$  expression, respectively.

We analyzed the biofilm formation of isogenic strains expressing green fluorescent protein (GFP) from the chromosome. These experiments were done in flow cells, and the biofilms were imaged using confocal laser scanning microscopy at 24, 48, and 72 h postinoculation (Fig. 4C). We used the quantitative analysis software COMSTAT (37) to calculate biomass, the average and maximum thickness, substratum coverage, and roughness of the biofilms at 72 h, when the differences in biofilm formation were most defined. The  $\Delta vxrA$  and  $\Delta vxrB$  strains formed visibly thinner biofilms compared with that of the wild type, with 1.5- to 1.6-fold decreases in biomass and average and

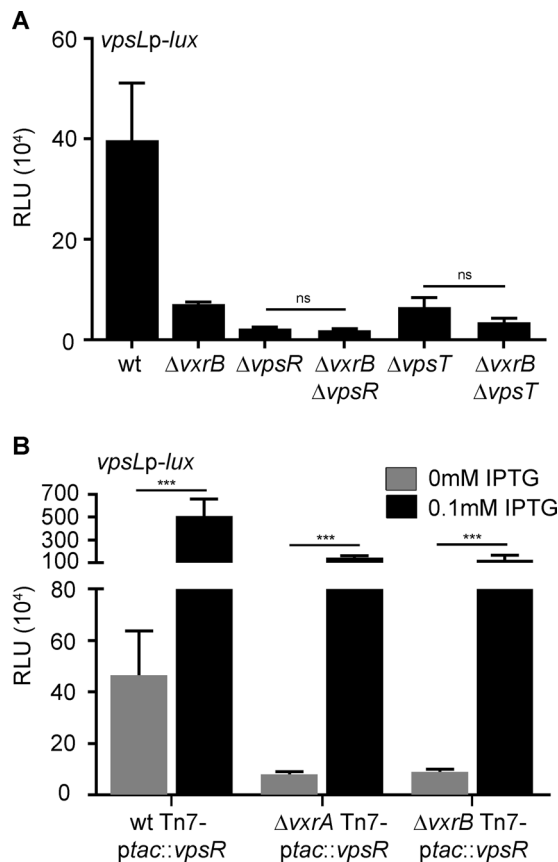


**FIG 3** Epistasis analysis of regulators of *vps* gene expression. (A) Cultures of wild-type,  $\Delta vxB$ ,  $\Delta vpsR$ ,  $\Delta vxB \Delta vpsR$ ,  $\Delta vpsT$ , and  $\Delta vxB \Delta vpsT$  strains containing  $P_{vpsL}$ -*lux* were grown to exponential phase ( $OD_{600}$  of  $\sim 0.3$ ) and luminescence was measured. The graph represents the averages and standard deviations of RLU obtained from three technical replicates from three biological replicates. RLU are reported in luminescence counts  $\cdot \text{min}^{-1} \cdot \text{ml}^{-1} \cdot OD_{600}^{-1}$ . Data were analyzed using a one-way analysis of variance (ANOVA) and Bonferroni's multiple-comparison test. ns, not significant. (B) Cultures of wild-type,  $\Delta vxA$ , and  $\Delta vxB$  strains containing  $P_{vpsL}$ -*lux* and an IPTG-inducible copy of *VpsR* in the Tn7 site were grown to exponential phase ( $OD_{600}$  of  $\sim 0.3$ ) and luminescence was measured. The graph represents the averages and standard deviations of RLU obtained from three technical replicates from three biological replicates. RLU are reported in luminescence counts  $\cdot \text{min}^{-1} \cdot \text{ml}^{-1} \cdot OD_{600}^{-1}$ . Data were analyzed using two-tailed Student's *t* tests. \*\*\*,  $P < 0.0001$ .

maximum thickness compared with that of the wild type (Table 1). By contrast, the  $\Delta vxC$  strain showed significantly increased biofilm formation compared with that of the wild type, and biomass and average thickness were both increased by 1.4-fold, while the maximum thickness increased by 1.3-fold (Table 1). The  $\Delta vxD$  and  $\Delta vxE$  strains formed biofilms similar to that of the wild type (Fig. 4B and C; Table 1). Since the  $\Delta vxA$ ,  $\Delta vxB$ , and  $\Delta vxC$  strains formed biofilms that were significantly different from that of the wild type, we generated  $\Delta vxA$ ,  $\Delta vxB$ , and  $\Delta vxC$  strains harboring *vxA*, *vxB*, and *vxC*, respectively, under the control of their own promoters ( $P_{vxA}$ ) in the Tn7 site and found that in these strains, *vpsL* expression was similar to that in the wild type (Fig. 4D). We next analyzed the genetic interaction between *vxC* and *vxB* with respect to the regulation of biofilm formation. The  $\Delta vxB$  and  $\Delta vxC$  strains showed decreased and increased *vpsL* expression, respectively, compared to that in the wild type. The  $\Delta vxB \Delta vxC$  strain phenocopied the *vpsL* expression level of the  $\Delta vxB$  strain, indicating that the  $\Delta vxB$  mutation is epistatic to the  $\Delta vxC$  mutation (Fig. 4E). Altogether, our results show that *VxA* and *VxB* both positively regulate *vpsL* expression and biofilm formation, while *VxC* may act as a repressor of biofilm formation. The roles of *VxD* and *VxE* in regulating biofilm formation are unclear, as both the  $\Delta vxD$  and  $\Delta vxE$  strains showed decreased *vpsL* expression but formed biofilms similar to that of the wild type.

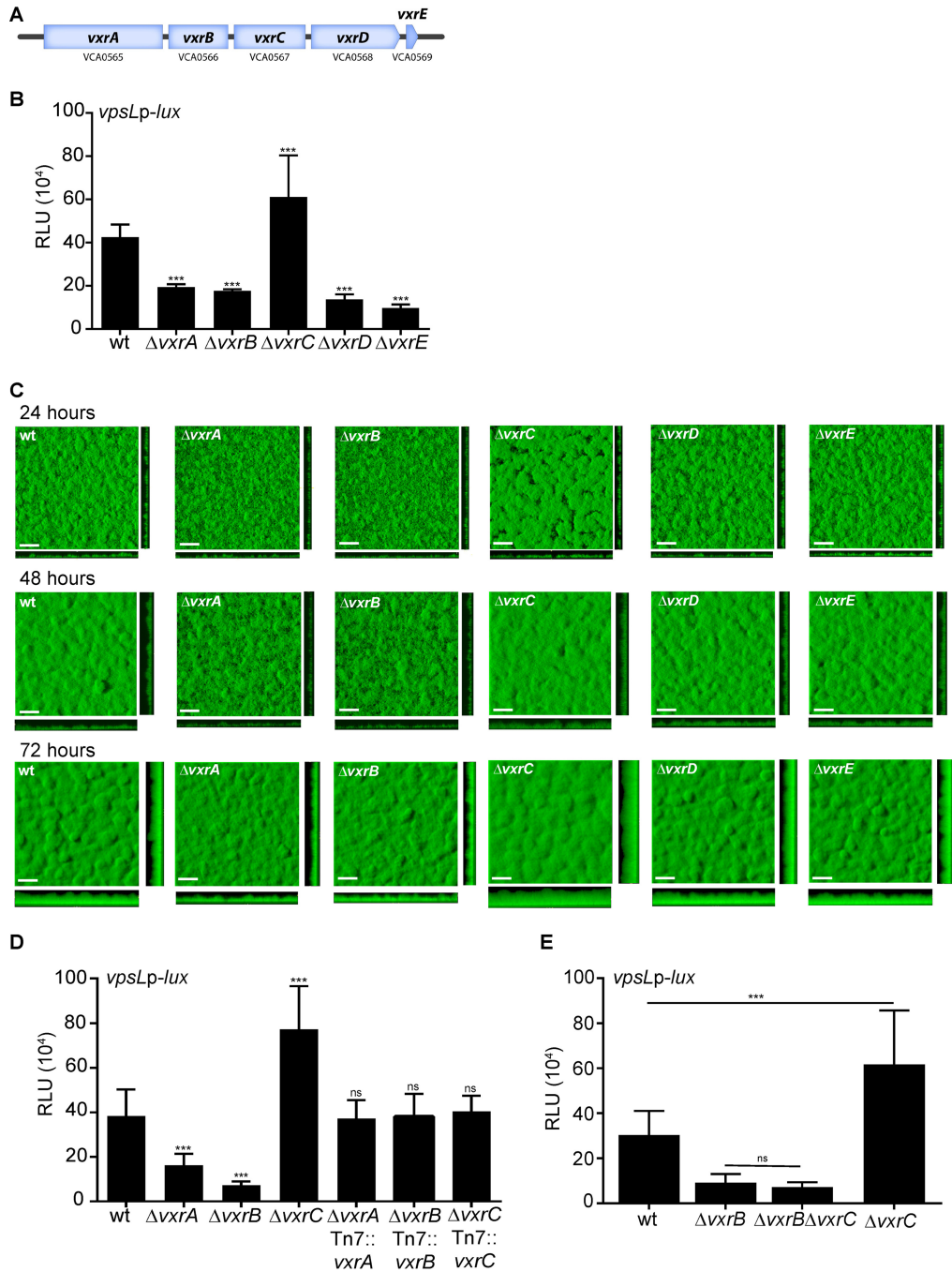


**FIG 4** Analysis of biofilm gene expression and biofilm formation in *vxr* operon mutants. (A) The 5-gene *vxr* operon structure, containing the TCS *vxrAB* and three genes of unknown function, *vxrCDE*. (B) Biofilms of the wild type and the  $\Delta vxrA$ ,  $\Delta vxrB$ ,  $\Delta vxrC$ ,  $\Delta vxrD$ , and  $\Delta vxrE$  strains containing  $P_{vpsL-lux}$  were grown in flow cells for 24 h, and luminescence was measured from harvested biofilm cells. The graph represents the averages and standard deviations of RLU obtained from three technical replicates from three independent biological samples. RLU are reported in luminescence counts  $\cdot$  min<sup>-1</sup>  $\cdot$  ml<sup>-1</sup>  $\cdot$   $\mu$ g<sup>-1</sup> total protein. Data were analyzed using a one-way analysis of variance (ANOVA) and Bonferroni's multiple-comparison test. \*\*\*,  $P < 0.001$ . (C) Top and orthogonal views of biofilms formed in flow cells by wild-type,  $\Delta vxrB$ ,  $\Delta vxrC$ ,  $\Delta vxrD$ , and  $\Delta vxrE$  strains 72 h after inoculation. Bars, 30  $\mu$ m. (D) Cultures of wild-type,  $\Delta vxrA$ ,  $\Delta vxrB$ ,  $\Delta vxrC$ ,  $\Delta vxrA$  Tn7::*vxrA*,  $\Delta vxrB$  Tn7::*vxrB*, and  $\Delta vxrC$  Tn7::*vxrC* strains containing  $P_{vpsL-lux}$  were grown to exponential phase ( $OD_{600}$  of  $\sim 0.3$ ) and luminescence was measured. The graph represents the averages and standard deviations of RLU obtained from three technical replicates from three independent biological replicates. RLU are reported in luminescence counts  $\cdot$  min<sup>-1</sup>  $\cdot$  ml<sup>-1</sup>  $\cdot$   $OD_{600}^{-1}$ . Data were analyzed using a one-way analysis of variance (ANOVA) and Bonferroni's multiple-comparison test. \*\*\*,  $P < 0.001$ ; ns, not significant. (E) Cultures of wild-type,  $\Delta vxrB$ ,  $\Delta vxrC$ , and  $\Delta vxrB \Delta vxrC$  strains containing  $P_{vpsL-lux}$  were grown to exponential phase ( $OD_{600}$  of  $\sim 0.3$ ) and luminescence was measured. The graph represents the averages and standard deviations of RLU obtained from three technical replicates from three independent biological replicates. RLU are reported in luminescence counts  $\cdot$  min<sup>-1</sup>  $\cdot$  ml<sup>-1</sup>  $\cdot$   $OD_{600}^{-1}$ . Data were analyzed using a one-way analysis of variance (ANOVA) and Bonferroni's multiple-comparison test. \*\*\*,  $P < 0.001$ .



**TABLE 1** COMSTAT analysis of biofilms of wild type,  $\Delta vxrA$ ,  $\Delta vxrB$ ,  $\Delta vxrC$ ,  $\Delta vxrD$ , and  $\Delta vxrE$  strains<sup>a</sup>

Time postinoculation and strain	Biomass ( $\mu\text{m}^3/\mu\text{m}^2$ [SD])	Mean thickness ( $\mu\text{m}$ [SD])		Substrate coverage <sup>b</sup> (SD)	Roughness coefficient (SD)
		Avg	Maximum		
24 h					
Wild type	7.77 (0.70)	8.53 (0.99)	14.00 (1.30)	0.90 (0.05)	0.23 (0.04)
$\Delta vxrA$ mutant	6.00 (0.79) <sup>d</sup>	6.38 (1.03)	12.67 (1.74)	0.87 (0.09)	0.28 (0.07)
$\Delta vxrB$ mutant	5.94 (0.73) <sup>d</sup>	6.25 (0.86) <sup>c</sup>	13.41 (1.30)	0.92 (0.05)	0.30 (0.08)
$\Delta vxrC$ mutant	8.73 (0.63)	9.43 (2.23)	14.44 (2.14)	0.91 (0.07)	0.23 (0.02)
$\Delta vxrD$ mutant	6.66 (0.84)	6.40 (0.94)	11.79 (1.55)	0.87 (0.19)	0.33 (0.16)
$\Delta vxrE$ mutant	7.087 (0.85)	7.88 (1.68)	13.26 (1.48)	0.87 (0.08)	0.25 (0.06)
48 h					
Wild type	10.94 (0.27)	12.12 (0.88)	22.84 (2.20)	0.91 (0.10)	0.14 (0.03)
$\Delta vxrA$ mutant	7.49 (1.02) <sup>e</sup>	8.31 (1.38) <sup>c</sup>	17.39 (2.89)	0.87 (0.21)	0.18 (0.05)
$\Delta vxrB$ mutant	8.35 (1.16) <sup>d</sup>	9.59 (1.59) <sup>c</sup>	20.18 (3.18)	0.91 (0.13)	0.20 (0.06)
$\Delta vxrC$ mutant	12.79 (2.35)	13.86 (2.94)	28.73 (7.43)	0.98 (0.03)	0.13 (0.04)
$\Delta vxrD$ mutant	11.06 (1.03)	12.49 (0.83)	22.10 (4.15)	0.93 (0.05)	0.15 (0.03)
$\Delta vxrE$ mutant	9.76 (1.30)	10.99 (0.59)	21.66 (3.78)	0.96 (0.06)	0.17 (0.03)
72 h					
Wild type	19.42 (1.49)	20.29 (1.25)	31.09 (2.20)	1.00 (0.00)	0.14 (0.03)
$\Delta vxrA$ mutant	11.58 (2.31) <sup>e</sup>	12.36 (2.18) <sup>e</sup>	21.22 (3.31) <sup>d</sup>	0.91 (0.07) <sup>c</sup>	0.19 (0.06)
$\Delta vxrB$ mutant	12.79 (2.08) <sup>d</sup>	14.61 (1.82) <sup>d</sup>	24.75 (2.44)	0.91 (0.07) <sup>c</sup>	0.21 (0.07) <sup>c</sup>
$\Delta vxrC$ mutant	26.34 (3.52) <sup>e</sup>	27.82 (3.29) <sup>e</sup>	40.07 (5.86) <sup>d</sup>	0.98 (0.04)	0.11 (0.03)
$\Delta vxrD$ mutant	18.95 (3.30)	19.61 (3.74)	30.35 (6.51)	0.98 (0.04)	0.13 (0.03)
$\Delta vxrE$ mutant	19.69 (3.15)	20.75 (4.13)	31.09 (4.79)	0.96 (0.07)	0.13 (0.03)

<sup>a</sup>Total biomass, the average and maximum thicknesses, substrate coverage, and roughness coefficient were calculated using COMSTAT. The values are the means (standard deviations) of data from at least six z-series image stacks. Significance was determined by ANOVA. Dunnett's multiple comparison test identified samples that differ significantly from biofilms formed by the wild-type strain.

<sup>b</sup>A value of 0 indicates no coverage (equivalent to 0%), while a value of 1 indicates full coverage (equivalent to 100%).

<sup>c</sup> $P \leq 0.05$ .

<sup>d</sup> $P \leq 0.001$ .

<sup>e</sup> $P \leq 0.0001$ .

**Overexpression of wild-type VxrB negatively impacts motility.** Biofilm formation and motility are inversely regulated in *V. cholerae*. Therefore, we analyzed the role of VxrB in the regulation of motility. We measured swimming motility of the  $\Delta vxrB$  strain by performing a motility assay on soft agar plates. We observed no difference in the average migration zone diameters between the  $\Delta vxrB$  and wild-type strains (Fig. 5A). To determine the effect that *vxrB* overexpression could have on motility, we cloned this gene in an expression plasmid under the control of an arabinose-inducible promoter (pBAD-*vxrB*). In the absence of arabinose, the migration zones of the wild type harboring the empty plasmid and the wild type containing pBAD-*vxrB* were similar (Fig. 5B). In the presence of 0.2% arabinose, the wild type containing pBAD-*vxrB* showed an ~50% decrease in migration compared with that of the wild type with the empty plasmid (Fig. 5B and C). These results suggest that overexpression of VxrB can impact motility.

**VxrB increases levels of the second messenger signaling molecule c-di-GMP.** Given VxrB's role as a positive regulator of biofilms and a negative regulator of motility, we asked if VxrB could be affecting cellular c-di-GMP levels, as this second messenger signaling molecule inversely regulates biofilms and motility. We measured intracellular c-di-GMP levels in wild-type,  $\Delta vxrA$ ,  $\Delta vxrB$ , and  $\Delta vxrC$  strains and found that  $\Delta vxrB$  and  $\Delta vxrC$  strains had small but statistically significant decreases in levels of c-di-GMP compared with that in the wild type, while the  $\Delta vxrA$  strain had c-di-GMP levels similar to that of the wild type (Fig. 6). Thus, cellular c-di-GMP levels are altered in the  $\Delta vxrB$  and  $\Delta vxrC$  strains.

**The T6SS does not impact *vpsL* expression or biofilm formation.** Our previous work indicated that VxrB positively regulates the T6SS (33). As biofilms provide an environment where cell-to-cell contact is frequent and where high activity of the T6SS might be expected, we next analyzed the role of the T6SS in biofilm formation and

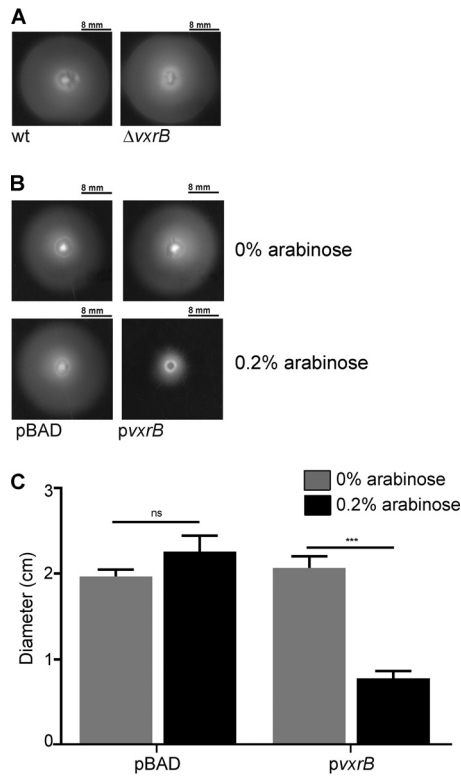


**FIG 5** Analysis of swimming motility in  $\Delta vxB$  and VxB overexpression strains. (A) Migration zones of wild-type and  $\Delta vxB$  strains after 16 h of growth on 0.3% agar plates. (B) Migration zones of the wild type expressing empty vector (pBAD) and pBAD-*vxB* (*pvxB*) after 16 h of growth on 0.3% agar plates containing 0% or 0.2% arabinose. (C) Strains were grown on LB agar plates containing 0.3% agar at 30°C for 16 h before migration zones were measured. The error bars indicate the standard deviations of the results from 6 biological replicates. Data were analyzed using two-tailed Student's *t* tests. \*\*\*,  $P < 0.0001$ .

determined if VxB's influence on biofilm formation could act partially through the regulation of, or activation by, the T6SS.

A strain lacking *hcp1* and *hcp2* ( $\Delta hcp1 \Delta hcp2$ ), the genes required to produce the major T6SS structural component, Hcp, was used to assess the role of the T6SS in biofilm formation (38). We also evaluated *vpsL* expression in cells grown to exponential phase in wild-type,  $\Delta vxB$ ,  $\Delta hcp1 \Delta hcp2$ , and  $\Delta vxB \Delta hcp1 \Delta hcp2$  strains (Fig. 7A). As

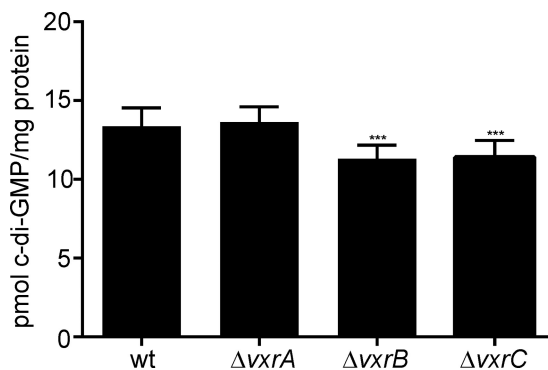


**FIG 6** Analysis of c-di-GMP levels in the wild type and in  $\Delta vxA$ ,  $\Delta vxB$ , and  $\Delta vxC$  mutants. Strains were grown aerobically to an  $OD_{600}$  of  $\sim 0.3$  before c-di-GMP was extracted from whole-cell protein and quantified by high-performance liquid chromatography-tandem mass spectrometry (HPLC-MS/MS). The error bars indicate the standard deviations of the results from 8 biological replicates. Data were analyzed using a one-way analysis of variance (ANOVA) and Bonferroni's multiple-comparison test. \*\*\*,  $P < 0.001$ .



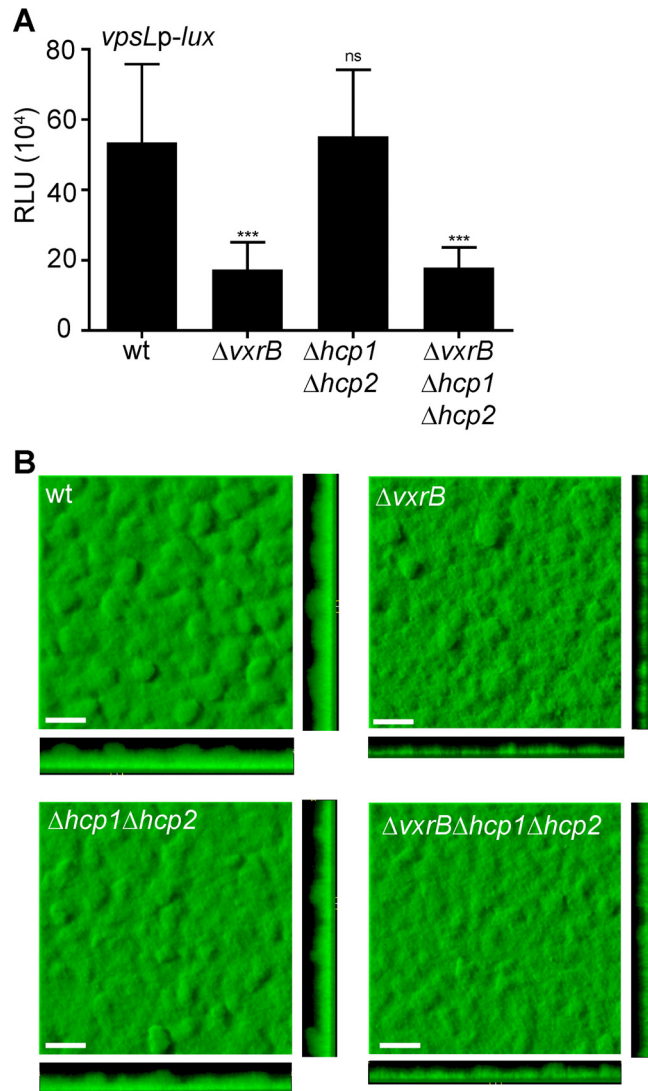


**FIG 7** Analysis of the impact of the type 6 secretion genes on biofilm gene expression and biofilm formation. (A) Cultures of wild-type,  $\Delta vxrB$ ,  $\Delta hcp1 \Delta hcp2$ , and  $\Delta vxrB \Delta hcp1 \Delta hcp2$  strains containing  $P_{vpsL}-lux$  were grown to exponential phase ( $OD_{600}$  of  $\sim 0.3$ ) and luminescence was measured. The graph represents the averages and standard deviations of RLU obtained from three technical replicates from three independent biological samples. RLU are reported in luminescence counts  $\cdot \text{min}^{-1} \cdot \text{ml}^{-1} \cdot OD_{600}^{-1}$ . Data were analyzed using a one-way analysis of variance (ANOVA) and Bonferroni's multiple-comparison test. \*\*\*,  $P < 0.001$ ; ns, not significant. (B) Top and orthogonal views of biofilms formed in flow cells by wild-type,  $\Delta vxrB$ ,  $\Delta hcp1 \Delta hcp2$ , and  $\Delta vxrB \Delta hcp1 \Delta hcp2$  strains after 72 h. Bars, 30  $\mu\text{m}$ .

expected, the  $\Delta vxrB$  strain demonstrated decreased *vpsL* expression, as did the  $\Delta vxrB \Delta hcp1 \Delta hcp2$  strain. The  $\Delta hcp1 \Delta hcp2$  strain showed no significant difference in *vpsL* expression compared with that of the wild type. Biofilm formation was also examined by growing strains expressing GFP in flow cells and imaging using confocal laser scanning microscopy at 72 h postinoculation (Fig. 7B). The  $\Delta vxrB$  and the  $\Delta vxrB \Delta hcp1 \Delta hcp2$  strains showed decreased biofilm formation, while the  $\Delta hcp1 \Delta hcp2$  strain showed no significant difference in biofilm formation compared with that of the wild type. These observations were supported by COMSTAT analysis, which was used to analyze biomass, the average and maximum thickness, substratum coverage, and roughness of biofilms (Table 2). Altogether, these findings indicate that the T6SS does not contribute to the regulation of biofilm formation by VxrB under the conditions we analyzed.

**TABLE 2** COMSTAT analysis of biofilms formed after 72 h by wild type,  $\Delta vxrB$ ,  $\Delta hcp12$ , and  $\Delta vxrB \Delta hcp1 \Delta hcp2$  strains<sup>a</sup>

Strain	Biomass ( $\mu\text{m}^3/\mu\text{m}^2$ [SD])	Mean thickness ( $\mu\text{m}$ [SD])		Substrate coverage <sup>b</sup> (SD)	Roughness coefficient (SD)
		Avg	Maximum		
Wild type	20.41 (2.63)	22 (3.34)	33.74 (6.084)	1.00 (00)	0.11 (0.02)
$\Delta vxrB$ mutant	11.68 (2.34) <sup>e</sup>	13.58 (2.12) <sup>e</sup>	23.48 (2.76) <sup>e</sup>	0.95 (0.05) <sup>c</sup>	0.21 (0.06) <sup>e</sup>
$\Delta hcp1 \Delta hcp2$ mutant	21.77 (0.73)	22.97 (0.88)	36.1 (2.65)	1.00 (00)	0.11 (0.02)
$\Delta vxrB \Delta hcp1 \Delta hcp2$ mutant	18.57 (2.82)	17.26 (1.68) <sup>d</sup>	27.70 (2.832) <sup>c</sup>	0.99 (0.02)	0.14 (0.01)

<sup>a</sup>Total biomass, the average and maximum thicknesses, substrate coverage, and roughness coefficient were calculated using COMSTAT. The values are the means (standard deviations) of data from at least six z-series image stacks. Significance was determined by ANOVA. Bonferroni's multiple-comparison test identified samples that differ significantly from biofilms formed by the wild-type strain.

<sup>b</sup>A value of 0 indicates no coverage (equivalent to 0%), while a value of 1 indicates full coverage (equivalent to 100%).

<sup>c</sup> $P \leq 0.05$ .

<sup>d</sup> $P \leq 0.001$ .

<sup>e</sup> $P \leq 0.0001$ .

**DISCUSSION**

*V. cholerae* biofilms enhance survival in the aquatic environment and facilitate transmission to a human host. This study serves to evaluate the role of TCSs, typically utilized to regulate cellular processes in response to extracellular signals, in biofilm formation. We systematically analyzed the role of *V. cholerae* RRs in biofilm formation and identified several that play roles in biofilm regulation (Fig. 8). Consistent with previous studies, we observed a decrease in *vpsL* expression in a  $\Delta vpsR$  (VC0665) mutant, a  $\Delta luxO$  (VC1021) mutant, and a  $\Delta vpsT$  (VCA0952) mutant and an increase in *vpsL* expression in a  $\Delta carR$  (VC1320) mutant (22, 24, 27, 28, 30). We did not observe a phenotype for a  $\Delta phoB$  (VC0719) mutant, which is only expected to act as repressor of biofilm formation under phosphate-limiting conditions (25, 26). As expected for the El Tor biotype, a  $\Delta vieA$  (VC1652) mutant did not have altered *vpsL* levels. In the classical

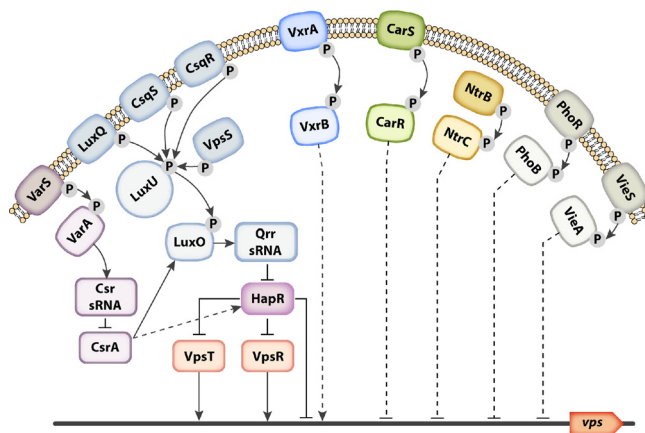


**FIG 8** Model of all known TCSs that regulate *V. cholerae* biofilm formation. The RRs VpsR (VC0665) and VpsT (VCA0952) are the major positive regulators of biofilm formation. Their cognate TCS partners have yet to be identified. The PhoB (VC0719-20) TCS acts as a repressor of biofilm formation under phosphate-limited conditions. LuxO (VC1021) acts as an activator of biofilm formation by positively regulating the expression of small regulatory RNAs responsible for repressing translation of *hapR*, the master quorum sensing regulator and the major negative regulator of biofilm formation. VarSA (VC2453/VC1213) represses biofilm formation by interfering with the LuxO-mediated activation of Qrr sRNAs through its activation of the inhibitory regulatory small RNAs CsrBCD and their subsequent inhibition of the global regulator CsrA. Repression of CsrA reduces Qrr sRNA levels, leading to increased HapR levels and decreased *vps* gene expression. CarSR (VC1319-20) negatively regulates biofilm formation. VieA (VC1652) represses biofilm formation independently of its cognate histidine kinase via an EAL domain responsible for degrading the secondary messenger c-di-GMP, an important positive regulator of biofilm formation. The NtrBC (VC2748-49) TCS was identified as a potential repressor of biofilms in this study. Although described in the text, VC1348 and VCA0210 are not pictured. These RRs contain HD-GYP domains responsible for degrading c-di-GMP. Although the deletion of these genes does not impact biofilm formation, their overexpression leads to a significant decrease in biofilm formation, indicating that they may act as repressors of biofilm formation. Finally, we have included the newly identified VxrAB (VCA0565-66) TCS, which positively regulates biofilm formation.

biotype of *V. cholerae*, *VieA* negatively regulates biofilms via an EAL domain, independently of its phosphorylation status and DNA-binding activity. The EAL domain functions as a phosphodiesterase (PDE) that degrades the secondary messenger *c*-di-GMP, an important positive regulator of biofilm formation (29). This phenotype is not observed in the El Tor biotype, as the transcription of *vieSAB* is subject to H-NS silencing (39, 40). We also did not observe a phenotype for the  $\Delta VC1348$  or  $\Delta VCA0210$  strain; however, this was also consistent with previously published findings, which demonstrated a biofilm phenotype only when these proteins were overexpressed (32).

Interestingly, we observed a 47-fold decrease in *vpsL* expression in the  $\Delta varA$  (VC1213) strain, which is contradictory to results from previously published work (31). The VarSA TCS is thought to impact biofilm formation through its control of levels of CsrA, a small RNA binding protein that regulates a number of cellular processes. Specifically, VarA is predicted to repress biofilm formation by interfering with the LuxO-mediated activation of Qrr sRNAs through its positive regulation of the inhibitory regulatory small RNAs CsrBCD. These small RNAs sequester CsrA, which in turn reduces Qrr sRNA levels, leading to increased HapR levels and decreased *vps* gene expression (41–44). However, a recent study demonstrated that the loss of VarA results in excessive levels of active CsrA, which negatively impacts cell growth and leads to single-amino-acid suppressor mutations in CsrA (45). These mutations were shown to alter the regulatory function of CsrA. Our sequence analysis of *csrA* in the  $\Delta varA$   $P_{vpsL}$ -*lux* strain revealed that this strain had an amino acid substitution of T11P. It was speculated by Mey et al. that the amino acid substitutions clustered in the N-terminal half of CsrA (R6H, R6L, T11P, I14T, and T19P) result in the accumulation of a “less active” form of CsrA (45). Thus, our finding is consistent with the observation that the loss of VarA results in suppressor mutations in *csrA* and that these mutations can alter CsrA activity, including its positive regulation of biofilm formation. Collectively, these observations explain why we did not observe the expected increase in *vpsL* expression in our  $\Delta varA$  strain. Although *varA* mutant strains do not produce the CsrA-sequestering sRNAs and have increased levels of the positive biofilm regulator, CsrA, we hypothesize that CsrA’s regulatory activity was altered due to the accumulation of a suppressor mutation. Finally, we found an increase in *vpsL* expression in a  $\Delta ntrC$  (VC2749) mutant, indicating that this RR may be a repressor of biofilm formation.

We focused our studies mainly on a new positive regulator of *vps* and biofilm formation, VxrB. The observations reported here demonstrate that VxrAB TCS activates biofilm formation and *vpsL* expression and represses motility. We showed that VxrB positively regulates *vpsR* and *vpsT*, the two major regulators of *V. cholerae* biofilms, and that VxrB regulates *vpsL* expression upstream of *VpsR* and *VpsT*. Finally, we demonstrated that VxrB positively regulates cellular levels of the second messenger signaling molecule *c*-di-GMP, which acts as a positive regulator of biofilm formation and a negative regulator of motility (46). While we demonstrated that VxrB may act through major biofilm regulators to exert its regulatory control on biofilm formation, further investigation of where VxrB is integrated into the *vps* regulatory network is necessary. It is possible that VxrB controls the activity of *vps* genes through its modulation of cellular *c*-di-GMP levels, as increased *c*-di-GMP levels have been shown to lead to increased *vpsL*, *vpsR*, and *vpsT* expression (39, 47). Alternatively, *VpsR* and *VpsT* may be the direct regulatory targets of VxrB, as both regulators positively regulate diguanylate cyclase (DGC) genes, which are responsible for producing *c*-di-GMP (48). Given that a VxrA mutant did not demonstrate a decrease in *c*-di-GMP levels and that a VxrC mutant had a decrease in *c*-di-GMP levels despite positively regulating biofilm formation, further investigation into the regulatory role of the Vxr TCS on *c*-di-GMP levels is merited. Determining the direct regulatory targets of VxrB would provide additional insight into our understanding of the role of TCS in the regulation and control of biofilm formation.

Our previous work demonstrated that *vxrABCDE* are cotranscribed and that *vxrCDE* have minor but significant roles in intestinal colonization (33). Here, we demonstrated that only the  $\Delta vxrA$ ,  $\Delta vxrB$ , and  $\Delta vxrC$  strains produced biofilms that were different from

that of the wild type, though  $\Delta vxrD$  and  $\Delta vxrE$  strains did demonstrate decreased *vpsL* expression. It is possible that VxrD and VxrE play minor roles in the activation of *vpsL* expression, potentially through the VxrAB pathway, but do not significantly impact biofilm formation. VxrC was shown to act as a repressor of *vpsL* expression and biofilm formation, and this phenotype was shown to be dependent on the presence of VxrB. This indicates that VxrC is in a pathway with the VxrAB TCS and that VxrC may interact with VxrA or VxrB to inhibit its regulation of biofilm formation. Further analysis of the Vxr operon members and their role in activating or repressing the VxrAB TCS will be essential for fully understanding the mechanism of action of this system.

c-di-GMP positively regulates biofilm formation and negatively regulates motility. Given the role of VxrAB in positively regulating biofilm formation and c-di-GMP levels, we investigated the impact of VxrB on motility. Our results demonstrated that deletion of *vxrB* did not impact motility but that overexpression of VxrB led to a decrease in motility. This is consistent with results from a previous study that demonstrated that overexpression of wild-type VxrB or constitutively active VxrB resulted in a loss of motility (36).

We have previously shown that VxrB is a positive regulator of the T6SS, a protein delivery system that requires cell-to-cell contact to translocate toxic effector proteins into a diverse group of target cells, including other bacteria, phagocytic amoebas, and human macrophages (33, 38, 49–51). In a biofilm, where cells are already in close contact, the T6SS could contribute to localized death and biofilm remodeling. The role of the T6SS in *V. cholerae* biofilms is unknown, and very few studies have been done in other species linking the T6SS to biofilm formation. In *Pseudomonas aeruginosa* strain PAO1, the structural component that makes up the inner sheath of the T6SS, Hcp, was shown to take part in the biofilm maturation stage (52). Additionally, a structural component of the outer sheath of the T6SS, *tssC1*, was demonstrated to promote antibiotic resistance in *P. aeruginosa* biofilms (53). In *Agrobacterium tumefaciens*, the ExoR regulator, an important regulator of biofilm formation, was shown to also regulate the T6SS, and in *Burkholderia cenocepacia*, a novel hybrid HK was identified that controls biofilm formation and the T6SS (54, 55). Thus, we wanted to determine the contribution of the T6SS on biofilm formation in *V. cholerae* and whether the decreased biofilm formation phenotype of the *vxrB* mutant is due to decreased T6SS activity. Our initial results indicate that the T6SS does not impact *V. cholerae* biofilm formation under the conditions tested. However, it is possible that under alternative growth conditions, the T6SS plays a structural or functional role within biofilms.

Determining the activating signals sensed by the VxrAB TCS will provide valuable insight into its mechanism of action. A recent study indicated that the VxrAB system may sense signals generated in response to  $\beta$ -lactam exposure, potentially either directly sensing the antibiotics themselves or sensing cell wall stress or degradation products (36). A VxrA homolog in *Vibrio parahaemolyticus*, VbrK, was shown to directly bind  $\beta$ -lactams to activate its cognate RR and stimulate the expression of a  $\beta$ -lactamase and additional  $\beta$ -lactam antibiotic resistance genes (56). Given that *V. cholerae* does not encode  $\beta$ -lactamase genes, it is interesting to consider the conditions under which VxrAB might encounter these potential signals and to speculate about the role they might play in directing the activity of this TCS. Subinhibitory concentrations of aminoglycoside antibiotics have been demonstrated to induce biofilm formation in *P. aeruginosa* and *Escherichia coli*, and it is possible that VxrAB mediates a similar response to  $\beta$ -lactam antibiotics in *V. cholerae* (57). Further investigation of the signals sensed by VxrAB is needed to fully elucidate the mechanism by which this TCS regulates diverse processes in *V. cholerae*.

It is evident that the VxrAB TCS plays an important regulatory role in *V. cholerae* and governs the T6SS, virulence, and cell wall homeostasis. This work identifies a new role for this system in biofilm formation and provides a better understanding of how VxrAB regulates important phases in the *V. cholerae* life cycle.

**TABLE 3** Bacterial strains and plasmids used in this study

Strain or plasmid	Relevant genotype	Source or reference
<i>E. coli</i> strains		
CC118 $\lambda$ pir	$\Delta$ ( <i>ara-leu</i> ) <i>araD</i> $\Delta$ <i>lacX74</i> <i>galE</i> <i>galk</i> <i>phoA20</i> <i>thi-1</i> <i>rpsE</i> <i>rpoB</i> <i>argE</i> (Am) <i>recA1</i> $\lambda$ pir	60
S17-1 $\lambda$ pir	Tp <sup>r</sup> Sm <sup>r</sup> <i>recA</i> <i>thi</i> <i>pro</i> r <sub>K</sub> <sup>-</sup> m <sub>K</sub> <sup>+</sup> RP4::2-Tc::MuKm Tn7 $\lambda$ pir	61
<i>V. cholerae</i> strains		
FY_VC_0001	O1 El Tor A1552, wild type, Rif <sup>r</sup>	62
FY_VC_0237	FY_VC_0001 mTn7 <i>gfp</i> Rif <sup>r</sup> Gm <sup>r</sup>	46
FY_VC_2272	$\Delta$ VCA0665 ( <i>vpsR</i> )	24
FY_VC_9332	$\Delta$ VCA0565 ( <i>vxrA</i> )	33
FY_VC_8758	$\Delta$ VCA0566 ( <i>vxrB</i> )	33
FY_VC_0099	$\Delta$ VCA0952 ( <i>vpsT</i> )	27
FY_VC_9369	$\Delta$ VCA0567 ( <i>vxrC</i> )	33
FY_VC_9417	$\Delta$ VCA0568 ( <i>vxrD</i> )	33
FY_VC_9394	$\Delta$ VCA0569 ( <i>vxrE</i> )	33
FY_VC_9469	$\Delta$ <i>vxrB</i> Tn7::v <i>xrB</i>	33
FY_VC_9952	$\Delta$ <i>vxrB</i> $\Delta$ <i>hcp1</i> $\Delta$ <i>hcp2</i>	33
FY_VC_9569	$\Delta$ VCA1415 $\Delta$ VCA0017 ( $\Delta$ <i>hcp1</i> $\Delta$ <i>hcp2</i> )	33
FY_VC_9390	$\Delta$ <i>vxrA</i> mTn7 <i>gfp</i> Rif <sup>r</sup> Gm <sup>r</sup>	This study
FY_VC_8764	$\Delta$ <i>vxrB</i> mTn7 <i>gfp</i> Rif <sup>r</sup> Gm <sup>r</sup>	This study
FY_VC_9392	$\Delta$ <i>vxrC</i> mTn7 <i>gfp</i> Rif <sup>r</sup> Gm <sup>r</sup>	This study
FY_VC_9437	$\Delta$ <i>vxrD</i> mTn7 <i>gfp</i> Rif <sup>r</sup> Gm <sup>r</sup>	This study
FY_VC_9439	$\Delta$ <i>vxrE</i> mTn7 <i>gfp</i> Rif <sup>r</sup> Gm <sup>r</sup>	This study
FY_VC_9234	$\Delta$ <i>vpsR</i> $\Delta$ <i>vxrB</i> Rif <sup>r</sup>	This study
FY_VC_9237	$\Delta$ <i>vpsT</i> $\Delta$ <i>vxrB</i> Rif <sup>r</sup>	This study
FY_VC_11356	FY_VC_0001 mTn7 P <sub>TAC</sub> - <i>vpsR</i> Rif <sup>r</sup> Gm <sup>r</sup>	This study
FY_VC_11357	$\Delta$ <i>vxrA</i> mTn7 P <sub>TAC</sub> - <i>vpsR</i> Rif <sup>r</sup> Gm <sup>r</sup>	This study
FY_VC_11358	$\Delta$ <i>vxrB</i> mTn7 P <sub>TAC</sub> - <i>vpsR</i> Rif <sup>r</sup> Gm <sup>r</sup>	This study
FY_VC_11355	$\Delta$ <i>vxrB</i> $\Delta$ <i>vxrC</i>	This study
FY_VC_12056	$\Delta$ <i>vxrA</i> -Tn7::v <i>xrA</i>	This study
FY_VC_12057	$\Delta$ <i>vxrC</i> -Tn7::v <i>xrC</i>	This study
Plasmids		
pGP704 <i>sacB</i> 28	pGP704 derivative, <i>mob/oriT sacB</i> Ap <sup>r</sup>	27
pUX-BF13	oriR6K helper plasmid, <i>mob/oriT</i> , provides the Tn7 transposition function in <i>trans</i> , Ap <sup>r</sup>	63
pMCM11	pGP704::mTn7 <i>gfp</i> Gm <sup>r</sup> Ap <sup>r</sup>	M. Miller and G. Schoolnik
pBBR <i>lux</i>	<i>luxCDABE</i> -based promoter fusion vector, Cm <sup>r</sup>	64
pFY-0950	pBBR <i>lux vpsL</i> promoter, Cm <sup>r</sup>	65
pFY-0989	pBBR <i>lux vpsR</i> promoter, Cm <sup>r</sup>	This study
pFY-0988	pBBR <i>lux vpsT</i> promoter, Cm <sup>r</sup>	This study
pBAD/myc His-B	Arabinose-inducible expression vector with C-terminal myc epitope and six-His tags	
pFY-2074	pBAD- <i>vxrB</i> -noTag Amp <sup>r</sup>	This study
pFY-3071	pBAD- <i>vxrB</i> <sup>D78A</sup> -noTag Amp <sup>r</sup>	This study
pFY-3073	pBAD- <i>vxrB</i> <sup>D78E</sup> -noTag Amp <sup>r</sup>	This study

## MATERIALS AND METHODS

**Strains and growth conditions.** All response regulator deletion strains used in Fig. 1 are listed in reference 33. Additional strains used in this study are listed in Table 3. *V. cholerae* and *Escherichia coli* strains were grown aerobically in Luria-Bertani (LB) broth (1% tryptone, 0.5% yeast extract, 1% NaCl, pH 7.5) at 30°C and 37°C, respectively. LB agar contained granulated agar (Difco) at 1.5% (wt/vol). Medium additives were used when necessary at the following concentrations: rifampin, 100  $\mu$ g/ $\mu$ l; ampicillin, 100  $\mu$ g/ $\mu$ l; and chloramphenicol, 20  $\mu$ g/ $\mu$ l for *E. coli* and 5  $\mu$ g/ $\mu$ l or 2.5  $\mu$ g/ $\mu$ l for *V. cholerae*.

**Strain and plasmid construction.** Plasmids were constructed using standard cloning methods or the Gibson Assembly recombinant DNA technique (New England Biolabs, Ipswich, MA). Gene deletions were carried out using allelic exchange of the native open reading frame (ORF) with the truncated ORF, as previously described (58). Complementation of  $\Delta$ *vxrB* was carried out using a Tn7-based system, as previously described (33). Briefly, triparental matings with donor *E. coli* S17 $\lambda$ pir carrying pGP704-Tn7 with the gene of interest, helper *E. coli* S17 $\lambda$ pir harboring pUX-BF13, and *V. cholerae* deletion strains were carried out by mixing all three strains and incubating mating mixtures on LB agar plates for 18 h at 30°C. Transconjugants were selected on thiosulfate-citrate-bile salts-sucrose (TCBS; BD Difco, Franklin Lakes, NJ) agar medium containing gentamicin (15  $\mu$ g/ $\mu$ l) at 30°C. Insertion of the complementation construct to the Tn7 site was verified by PCR. *V. cholerae* wild-type and mutant strains were tagged with the green fluorescent protein gene (*gfp*) according to a previously described procedure (14). The *gfp*-tagged *V. cholerae* strains were verified by PCR and used in biofilm analyses. Transcriptional fusions were constructed by cloning the upstream regulatory regions of selected genes into the pBBR-*lux* plasmid, as previously described (59).



**Luminescence assays from planktonically grown cells.** Overnight cultures of *V. cholerae* cells were diluted 1:500 in appropriate medium containing chloramphenicol (5  $\mu\text{g/ml}$ ). Cells were then grown aerobically at 30°C to an optical density at 600 nm ( $\text{OD}_{600}$ ) of 0.3 to 0.4, and then the luminescence of cells was measured using a PerkinElmer Victor3 multilabel counter (PerkinElmer, Waltham, MA). Lux expression is reported as counts  $\cdot \text{min}^{-1} \cdot \text{ml}^{-1} \cdot \text{OD}_{600}^{-1}$ , shown as relative light units (RLU). Assays were repeated with three biological replicates. Three technical replicates were measured for all assays. Statistical analysis was performed using one-way analysis of variance (ANOVA) and Bonferroni's multiple-comparison test.

**Luminescence assays from biofilm-grown cells.** Flow cells were inoculated by diluting overnight-grown cultures of *V. cholerae* cells harboring  $P_{\text{vpst}}\text{-lux}$  1:200 and injecting cells into an Ibidi m-Slide VI0.4 (Ibidi 80601; Ibidi LLC, Verona, WI). After inoculation, the bacteria were allowed to adhere at room temperature for 1 h with no flow. Next, the flow of 2% (vol/vol) LB (0.2 g/liter tryptone, 0.1 g/liter yeast extract, 1% NaCl) containing chloramphenicol (2.5  $\mu\text{g/ml}$ ) was initiated at a rate of 7.5 ml/h and continued for up to 24 h at 25°C. After 24 h, biofilms were harvested in 1 ml phosphate-buffered saline (PBS) for luminescence reading. The luminescence of cells was read using a PerkinElmer Victor3 multilabel counter (PerkinElmer, Waltham, MA) and is reported as counts  $\cdot \text{min}^{-1} \cdot \text{ml}^{-1} \cdot \mu\text{g}^{-1}$  protein concentration, as calculated by the bicinchoninic acid (BCA) assay (Thermo Fisher, Waltham, MA) using bovine serum albumin (BSA) as standards. Lux expression is reported as relative light units (RLU). Assays were repeated with two biological replicates, and three technical replicates were measured for all assays. Statistical analysis was performed using ANOVA and Bonferroni's multiple-comparison test.

**Biofilm assays.** Flow cells were inoculated by diluting overnight-grown cultures of *gfp*-tagged *V. cholerae* strains 1:200 ( $\text{OD}_{600}$  of 0.02) and injecting cells into an Ibidi m-Slide VI0.4 (Ibidi 80601; Ibidi LLC, Verona, WI). After inoculation, the bacteria were allowed to adhere at room temperature for 1 h with no flow. Next, the flow of 2% (vol/vol) LB (0.2 g/liter tryptone, 0.1 g/liter yeast extract, 1% NaCl) was initiated at a rate of 7.5 ml/h and continued for up to 72 h. Confocal laser scanning microscopy (CLSM) images of the biofilms were captured with an LSM 5 PASCAL system (Zeiss) using an excitation wavelength of 488 nm and an emission wavelength of 543 nm. Three-dimensional images of the biofilms were reconstructed using Imaris software (Bitplane) and quantified using COMSTAT 2 (37). Statistical analysis of COMSTAT data was performed using ANOVA and Bonferroni's multiple-comparison test.

**Motility assays.** Soft agar motility plates were made using LB medium with 0.3% (wt/vol) agar supplemented with 100  $\mu\text{g}/\mu\text{l}$  ampicillin or 100  $\mu\text{g}/\mu\text{l}$  ampicillin and 0.1 mM IPTG. The plates were inoculated by stabbing the agar from an overnight colony of the strains to be tested. The plates were then incubated at 30°C. Diameters of the migration zones were measured after 16 h. Statistical analysis was performed using ANOVA and Bonferroni's multiple-comparison test.

**Determination of intracellular c-di-GMP levels.** c-di-GMP extraction was performed as previously described (58). Briefly, *V. cholerae* wild-type,  $\Delta\text{vxrB}$ ,  $\Delta\text{vxrC}$ , and  $\Delta\text{vxrB}$  Tn7::*vxrB*-complemented strains were grown in LB broth to an  $\text{OD}_{600}$  of 0.4 before 40 ml of culture was harvested at  $4,000 \times g$  for 30 min. Cell pellets were allowed to dry briefly and then resuspended in 1 ml extraction solution (40% acetonitrile, 40% methanol, 0.1% formic acid, 19.9% high-pressure liquid chromatography [HPLC]-grade water), and incubated on ice for 15 min. Samples were then centrifuged at  $16,000 \times g$  for 5 min and 800  $\mu\text{l}$  of supernatant was dried under vacuum and then lyophilized. Samples were resuspended in 50  $\mu\text{l}$  of 184 mM NaCl and analyzed by liquid chromatography-tandem mass spectrometry (LC-MS/MS) on a Thermo-Electron Finnigan LTQ mass spectrometer coupled to a surveyor HPLC. The amount of c-di-GMP in samples was calculated with a standard curve generated from pure c-di-GMP suspended in 184 mM NaCl (Biolog Life Science Institute, Bremen, Germany). The concentrations used for the standard curve generation were 50 nM, 100 nM, 500 nM, 2  $\mu\text{M}$ , 3.5  $\mu\text{M}$ , 5  $\mu\text{M}$ , 7.5  $\mu\text{M}$ , and 10  $\mu\text{M}$ . The assay is linear from 50 nM to 10  $\mu\text{M}$ , with an  $R^2$  of 0.999. The c-di-GMP levels were normalized to total protein per ml of culture.

To determine protein concentration, 4 ml from each culture was harvested, the supernatant was removed, and cells were lysed in 1 ml of 2% sodium dodecyl sulfate (SDS). Total protein in the samples was determined with a bicinchoninic acid (BCA) assay (Thermo Fisher, Waltham, MA) using bovine serum albumin (BSA) as the standard. Each c-di-GMP quantification experiment was performed with four biological replicates. Statistical analysis was performed using ANOVA and Bonferroni's multiple-comparison test.

## ACKNOWLEDGMENTS

We thank Benjamin Abrams from the UCSC Life Sciences Microscopy Center for his technical support, Qiangli Zhang for help with the high-performance liquid chromatography-tandem mass spectrometry (HPLC-MS/MS) experiments and analysis, Ates Gurcan for his assistance with Fig. 8, and David Zamorano-Sánchez for his comments on the manuscript.

This work was supported by the NIH grant R01AI055987 to F.H.Y.

## REFERENCES

- Kaper JB, Morris JG, Levine MM. 1995. Cholera. Clin Microbiol Rev 8:48–86.
- Faruque SM, Albert MJ, Mekalanos JJ. 1998. Epidemiology, genetics, and ecology of toxigenic *Vibrio cholerae*. Microbiol Mol Biol Rev 62:1301–1314.
- Charles RC, Ryan ET. 2011. Cholera in the 21st century. Curr Opin Infect Dis 24:472–477. <https://doi.org/10.1097/QCO.0b013e32834a88af>.
- Teschler JK, Zamorano-Sánchez D, Utada AS, Warner CJA, Wong GCL, Linington RG, Yildiz FH. 2015. Living in the matrix: assembly and control of *Vibrio cholerae* biofilms. Nat Rev Microbiol 13:255–268. <https://doi.org/10.1038/nrmicro3433>.
- Islam MS, Jahid MIK, Rahman MM, Rahman MZ, Islam MS, Kabir MS, Sack DA, Schoolnik GK. 2007. Biofilm acts as a microenvironment for



- plankton-associated *Vibrio cholerae* in the aquatic environment of Bangladesh. *Microbiol Immunol* 51:369–379. <https://doi.org/10.1111/j.1348-0421.2007.tb03924.x>.
6. Faruque SM, Biswas K, Udden SMN, Ahmad QS, Sack DA, Nair GB, Mekalanos JJ. 2006. Transmissibility of cholera: *in vivo*-formed biofilms and their relationship to infectivity and persistence in the environment. *Proc Natl Acad Sci U S A* 103:6350–6355. <https://doi.org/10.1073/pnas.0601277103>.
  7. Alam M, Sultana M, Nair GB, Siddique AK, Hasan NA, Sack RB, Sack DA, Ahmed KU, Sadique A, Watanabe H, Grim CJ, Huq A, Colwell RR. 2007. Viable but nonculturable *Vibrio cholerae* O1 in biofilms in the aquatic environment and their role in cholera transmission. *Proc Natl Acad Sci U S A* 104:17801–17806. <https://doi.org/10.1073/pnas.0705599104>.
  8. Conner JG, Teschler JK, Jones CJ, Yildiz FH. 2016. Staying alive: *Vibrio cholerae*'s cycle of environmental survival, transmission, and dissemination. *Microbiol Spectr* 4:VMBF-0015-2015. <https://doi.org/10.1128/microbiolspec.VMBF-0015-2015>.
  9. Nielsen AT, Dolganov NA, Rasmussen T, Otto G, Miller MC, Felt SA, Torreilles S, Schoolnik GK. 2010. A bistable switch and anatomical site control *Vibrio cholerae* virulence gene expression in the intestine. *PLoS Pathog* 6:e1001102. <https://doi.org/10.1371/journal.ppat.1001102>.
  10. Berk V, Fong JCN, Dempsey GT, Develioglu ON, Zhuang X, Liphardt J, Yildiz FH, Chu S. 2012. Molecular architecture and assembly principles of *Vibrio cholerae* biofilms. *Science* 337:236–239. <https://doi.org/10.1126/science.1222981>.
  11. Absalon C, Van Dellen K, Watnick PI. 2011. A communal bacterial adhesin anchors biofilm and bystander cells to surfaces. *PLoS Pathog* 7:e1002210. <https://doi.org/10.1371/journal.ppat.1002210>.
  12. Fong JCN, Syed KA, Klose KE, Yildiz FH. 2010. Role of *Vibrio* polysaccharide (*vps*) genes in VPS production, biofilm formation and *Vibrio cholerae* pathogenesis. *Microbiology* 156:2757–2769. <https://doi.org/10.1099/mic.0.040196-0>.
  13. Yildiz FH, Schoolnik GK. 1999. *Vibrio cholerae* O1 El Tor: identification of a gene cluster required for the rugose colony type, exopolysaccharide production, chlorine resistance, and biofilm formation. *Proc Natl Acad Sci U S A* 96:4028–4033. <https://doi.org/10.1073/pnas.96.7.4028>.
  14. Fong JCN, Karplus K, Schoolnik GK, Yildiz FH. 2006. Identification and characterization of RbmA, a novel protein required for the development of rugose colony morphology and biofilm structure in *Vibrio cholerae*. *J Bacteriol* 188:1049–1059. <https://doi.org/10.1128/JB.188.3.1049-1059.2006>.
  15. Fong JCN, Yildiz FH. 2007. The *rbmBCDEF* gene cluster modulates development of rugose colony morphology and biofilm formation in *Vibrio cholerae*. *J Bacteriol* 189:2319–2330. <https://doi.org/10.1128/JB.01569-06>.
  16. Moorthy S, Watnick PI. 2005. Identification of novel stage-specific genetic requirements through whole genome transcription profiling of *Vibrio cholerae* biofilm development. *Mol Microbiol* 57:1623–1635. <https://doi.org/10.1111/j.1365-2958.2005.04797.x>.
  17. Yildiz FH, Visick KL. 2009. *Vibrio* biofilms: so much the same yet so different. *Trends Microbiol* 17:109–118. <https://doi.org/10.1016/j.tim.2008.12.004>.
  18. Townsley L, Sison Mangus MP, Mehic S, Yildiz FH. 2016. Response of *Vibrio cholerae* to low-temperature shift: CpsV regulates type VI secretion, biofilm formation, and association with zooplankton. *Appl Environ Microbiol* 82:e00807-16. <https://doi.org/10.1128/AEM.00807-16>.
  19. Shikuma NJ, Yildiz FH. 2009. Identification and characterization of OsrR, a transcriptional regulator involved in osmolarity adaptation in *Vibrio cholerae*. *J Bacteriol* 191:4082–4096. <https://doi.org/10.1128/JB.01540-08>.
  20. Beier D, Gross R. 2006. Regulation of bacterial virulence by two-component systems. *Curr Opin Microbiol* 9:143–152. <https://doi.org/10.1016/j.mib.2006.01.005>.
  21. Calva E, Oropeza R. 2006. Two-component signal transduction systems, environmental signals, and virulence. *Microb Ecol* 51:166–176. <https://doi.org/10.1007/s00248-005-0087-1>.
  22. Bilecen K, Yildiz FH. 2009. Identification of a calcium-controlled negative regulatory system affecting *Vibrio cholerae* biofilm formation. *Environ Microbiol* 11:2015–2029. <https://doi.org/10.1111/j.1462-2920.2009.01923.x>.
  23. Shikuma NJ, Davis KR, Fong JCN, Yildiz FH. 2013. The transcriptional regulator, CosR, controls compatible solute biosynthesis and transport, motility and biofilm formation in *Vibrio cholerae*. *Environ Microbiol* 15:1387–1399. <https://doi.org/10.1111/j.1462-2920.2012.02805.x>.
  24. Yildiz FH, Dolganov NA, Schoolnik GK. 2001. VpsR, a member of the response regulators of the two-component regulatory systems, is required for expression of *vps* biosynthesis genes and EPS(ET)-associated phenotypes in *Vibrio cholerae* O1 El Tor. *J Bacteriol* 183:1716–1726. <https://doi.org/10.1128/JB.183.5.1716-1726.2001>.
  25. Pratt JT, McDonough E, Camilli A. 2009. PhoB regulates motility, biofilms, and cyclic di-GMP in *Vibrio cholerae*. *J Bacteriol* 191:6632–6642. <https://doi.org/10.1128/JB.00708-09>.
  26. Sultan SZ, Silva AJ, Benitez JA. 2010. The PhoB regulatory system modulates biofilm formation and stress response in El Tor biotype *Vibrio cholerae*. *FEMS Microbiol Lett* 302:22–31. <https://doi.org/10.1111/j.1574-6968.2009.01837.x>.
  27. Casper-Lindley C, Yildiz FH. 2004. VpsT is a transcriptional regulator required for expression of *vps* biosynthesis genes and the development of rugose colonial morphology in *Vibrio cholerae* O1 El Tor. *J Bacteriol* 186:1574–1578. <https://doi.org/10.1128/JB.186.5.1574-1578.2004>.
  28. Hammer BK, Bassler BL. 2003. Quorum sensing controls biofilm formation in *Vibrio cholerae*. *Mol Microbiol* 50:101–104. <https://doi.org/10.1046/j.1365-2958.2003.03688.x>.
  29. Tischler AD, Camilli A. 2004. Cyclic diguanylate (c-di-GMP) regulates *Vibrio cholerae* biofilm formation. *Mol Microbiol* 53:857–869. <https://doi.org/10.1111/j.1365-2958.2004.04155.x>.
  30. Bilecen K, Fong JCN, Cheng A, Jones CJ, Zamorano-Sánchez D, Yildiz FH. 2015. Polymyxin B resistance and biofilm formation in *Vibrio cholerae* is controlled by the response regulator CarR. *Infect Immun* 83:1199–1209. <https://doi.org/10.1128/IAI.02700-14>.
  31. Lenz DH, Miller MB, Zhu J, Kulkarni RV, Bassler BL. 2005. CsrA and three redundant small RNAs regulate quorum sensing in *Vibrio cholerae*. *Mol Microbiol* 58:1186–1202. <https://doi.org/10.1111/j.1365-2958.2005.04902.x>.
  32. McKee RW, Kariisa A, Mudrak B, Whitaker C, Tamayo R. 2014. A systematic analysis of the *in vitro* and *in vivo* functions of the HD-GYP domain proteins of *Vibrio cholerae*. *BMC Microbiol* 14:272. <https://doi.org/10.1186/s12866-014-0272-9>.
  33. Cheng AT, Ottemann KM, Yildiz FH. 2015. *Vibrio cholerae* response regulator VxrB controls colonization and regulates the type VI secretion system. *PLoS Pathog* 11:e1004933. <https://doi.org/10.1371/journal.ppat.1004933>.
  34. Butler SM, Camilli A. 2005. Going against the grain: chemotaxis and infection in *Vibrio cholerae*. *Nat Rev Microbiol* 3:611–620. <https://doi.org/10.1038/nrmicro1207>.
  35. Butler SM, Camilli A. 2004. Both chemotaxis and net motility greatly influence the infectivity of *Vibrio cholerae*. *Proc Natl Acad Sci U S A* 101:5018–5023. <https://doi.org/10.1073/pnas.0308052101>.
  36. Dörr T, Alvarez L, Delgado F, Davis BM, Cava F, Waldor MK. 2016. A cell wall damage response mediated by a sensor kinase/response regulator pair enables beta-lactam tolerance. *Proc Natl Acad Sci U S A* 113:404–409. <https://doi.org/10.1073/pnas.1520333113>.
  37. Heydorn A, Nielsen AT, Hentzer M, Sternberg C, Givskov M, Ersbøll BK, Molin S. 2000. Quantification of biofilm structures by the novel computer program COMSTAT. *Microbiology* 146 (Pt 10):2395–2407. <https://doi.org/10.1099/00221287-146-10-2395>.
  38. Pukatzki S, Ma AT, Sturtevant D, Krastins B, Sarracino D, Nelson WC, Heidelberg JF, Mekalanos JJ. 2006. Identification of a conserved bacterial protein secretion system in *Vibrio cholerae* using the *Dictyostelium* host model system. *Proc Natl Acad Sci U S A* 103:1528–1533. <https://doi.org/10.1073/pnas.0510322103>.
  39. Beyhan S, Tischler AD, Camilli A, Yildiz FH. 2006. Differences in gene expression between the classical and El Tor biotypes of *Vibrio cholerae* O1. *Infect Immun* 74:3633–3642. <https://doi.org/10.1128/IAI.01750-05>.
  40. Wang H, Ayala JC, Benitez JA, Silva AJ. 2015. RNA-Seq analysis identifies new genes regulated by the histone-like nucleoid structuring protein (H-NS) affecting *Vibrio cholerae* virulence, stress response and chemotaxis. *PLoS One* 10:e0118295. <https://doi.org/10.1371/journal.pone.0118295>.
  41. Lenz DH, Mok KC, Lilley BN, Kulkarni RV, Wingreen NS, Bassler BL. 2004. The small RNA chaperone Hfq and multiple small RNAs control quorum sensing in *Vibrio harveyi* and *Vibrio cholerae*. *Cell* 118:69–82. <https://doi.org/10.1016/j.cell.2004.06.009>.
  42. Tsou AM, Liu Z, Cai T, Zhu J. 2011. The VarS/VarA two-component system modulates the activity of the *Vibrio cholerae* quorum-sensing transcriptional regulator HapR. *Microbiology* 157:1620–1628. <https://doi.org/10.1099/mic.0.046235-0>.
  43. Jang J, Jung K-T, Yoo C-K, Rhie G-E. 2010. Regulation of hemagglutinin/protease expression by the VarS/VarA-CsrA/B/C/D system in *Vibrio cholerae*. *Microb Pathog* 48:245–250. <https://doi.org/10.1016/j.micpath.2010.03.003>.

44. Jang J, Jung K-T, Park J, Yoo C-K, Rhie G-E. 2011. The *Vibrio cholerae* Var5/VarA two-component system controls the expression of virulence proteins through ToxT regulation. *Microbiology* 157:1466–1473. <https://doi.org/10.1099/mic.0.043737-0>.
45. Mey AR, Butz HA, Payne SM. 2015. *Vibrio cholerae* CsrA regulates ToxR levels in response to amino acids and is essential for virulence. *mBio* 6:e01064. <https://doi.org/10.1128/mBio.01064-15>.
46. Beyhan S, Tischler AD, Camilli A, Yildiz FH. 2006. Transcriptome and phenotypic responses of *Vibrio cholerae* to increased cyclic di-GMP level. *J Bacteriol* 188:3600–3613. <https://doi.org/10.1128/JB.188.10.3600-3613.2006>.
47. Krasteva PV, Fong JCN, Shikuma NJ, Beyhan S, Navarro MVA, Yildiz FH, Sondermann H. 2010. *Vibrio cholerae* VpsT regulates matrix production and motility by directly sensing cyclic di-GMP. *Science* 327:866–868. <https://doi.org/10.1126/science.1181185>.
48. Beyhan S, Bilecen K, Salama SR, Casper-Lindley C, Yildiz FH. 2007. Regulation of rugosity and biofilm formation in *Vibrio cholerae*: comparison of VpsT and VpsR regulons and epistasis analysis of *vpsT*, *vpsR*, and *hapR*. *J Bacteriol* 189:388–402. <https://doi.org/10.1128/JB.00981-06>.
49. Zheng J, Ho B, Mekalanos JJ. 2011. Genetic analysis of anti-amoebae and anti-bacterial activities of the type VI secretion system in *Vibrio cholerae*. *PLoS One* 6:e23876. <https://doi.org/10.1371/journal.pone.0023876>.
50. Pukatzki S, Ma AT, Revel AT, Sturtevant D, Mekalanos JJ. 2007. Type VI secretion system translocates a phage tail spike-like protein into target cells where it cross-links actin. *Proc Natl Acad Sci U S A* 104:15508–15513. <https://doi.org/10.1073/pnas.0706532104>.
51. MacIntyre DL, Miyata ST, Kitaoka M, Pukatzki S. 2010. The *Vibrio cholerae* type VI secretion system displays antimicrobial properties. *Proc Natl Acad Sci U S A* 107:19520–19524. <https://doi.org/10.1073/pnas.1012931107>.
52. Southey-Pillig CJ, Davies DG, Sauer K. 2005. Characterization of temporal protein production in *Pseudomonas aeruginosa* biofilms. *J Bacteriol* 187:8114–8126. <https://doi.org/10.1128/JB.187.23.8114-8126.2005>.
53. Zhang L, Hinz AJ, Nadeau J-P, Mah T-F. 2011. *Pseudomonas aeruginosa* *tssC1* links type VI secretion and biofilm-specific antibiotic resistance. *J Bacteriol* 193:5510–5513. <https://doi.org/10.1128/JB.00268-11>.
54. Heckel BC, Tomlinson AD, Morton ER, Choi J-H, Fuqua C. 2014. *Agrobacterium tumefaciens* *exoR* controls acid response genes and impacts exopolysaccharide synthesis, horizontal gene transfer, and virulence gene expression. *J Bacteriol* 196:3221–3233. <https://doi.org/10.1128/JB.01751-14>.
55. Aubert DF, Flannagan RS, Valvano MA. 2008. A novel sensor kinase response regulator hybrid controls biofilm formation and type VI secretion system activity in *Burkholderia cenocepacia*. *Infect Immun* 76:1979–1991. <https://doi.org/10.1128/IAI.01338-07>.
56. Li L, Wang Q, Zhang H, Yang M, Khan MI, Zhou X. 2016. Sensor histidine kinase is a  $\beta$ -lactam receptor and induces resistance to  $\beta$ -lactam antibiotics. *Proc Natl Acad Sci U S A* 113:1648–1653. <https://doi.org/10.1073/pnas.1520300113>.
57. Hoffman LR, D'Argenio DA, MacCoss MJ, Zhang Z, Jones RA, Miller SI. 2005. Aminoglycoside antibiotics induce bacterial biofilm formation. *Nature* 436:1171–1175. <https://doi.org/10.1038/nature03912>.
58. Liu X, Beyhan S, Lim B, Linington RG, Yildiz FH. 2010. Identification and characterization of a phosphodiesterase that inversely regulates motility and biofilm formation in *Vibrio cholerae*. *J Bacteriol* 192:4541–4552. <https://doi.org/10.1128/JB.00209-10>.
59. Zamorano-Sánchez D, Fong JCN, Kilic S, Erill I, Yildiz FH. 2015. Identification and characterization of VpsR and VpsT binding sites in *Vibrio cholerae*. *J Bacteriol* 197:1221–1235. <https://doi.org/10.1128/JB.02439-14>.
60. Herrero M, de Lorenzo V, Timmis KN. 1990. Transposon vectors containing non-antibiotic resistance selection markers for cloning and stable chromosomal insertion of foreign genes in gram-negative bacteria. *J Bacteriol* 172:6557–6567. <https://doi.org/10.1128/jb.172.11.6557-6567.1990>.
61. de Lorenzo V, Timmis KN. 1994. Analysis and construction of stable phenotypes in gram-negative bacteria with Tn5- and Tn10-derived mini-transposons. *Methods Enzymol* 235:386–405. [https://doi.org/10.1016/0076-6879\(94\)35157-0](https://doi.org/10.1016/0076-6879(94)35157-0).
62. Yildiz FH, Schoolnik GK. 1998. Role of *rpoS* in stress survival and virulence of *Vibrio cholerae*. *J Bacteriol* 180:773–784.
63. Bao Y, Lies DP, Fu H, Roberts GP. 1991. An improved Tn7-based system for the single-copy insertion of cloned genes into chromosomes of Gram-negative bacteria. *Gene* 109:167–168. [https://doi.org/10.1016/0378-1119\(91\)90604-A](https://doi.org/10.1016/0378-1119(91)90604-A).
64. Hammer BK, Bassler BL. 2007. Regulatory small RNAs circumvent the conventional quorum sensing pathway in pandemic *Vibrio cholerae*. *Proc Natl Acad Sci U S A* 104:11145–11149. <https://doi.org/10.1073/pnas.0703860104>.
65. Shikuma NJ, Fong JCN, Yildiz FH. 2012. Cellular levels and binding of c-di-GMP control subcellular localization and activity of the *Vibrio cholerae* transcriptional regulator VpsT. *PLoS Pathog* 8:e1002719. <https://doi.org/10.1371/journal.ppat.1002719>.